Making Graphene Visible on Transparent Dielectric Substrates: Brewster Angle Imaging

Priscila Romagnoli[1]; Henrique G. Rosa[1]; Daniel Lopez-Cortes[1]; Eunézio A. T. Souza[1]; José C. Viana-Gomes[2]; Walter Margulis[3]; Christiano J. S. de Matos[1]

[1]MackGraphe - Graphene and Nanomaterials Research Center, Mackenzie Presbyterian University, Sao Paulo, 01302-907, Brazil

[2]Center for Advanced 2D Materials and Graphene Research Center, National University of Singapore, 117542, Singapore

[3]Acreo Swedish ICT AB, Stockholm, 164 40, Sweden

E-mail: cjsdematos@mackenzie.br

Abstract. The visibility of graphene is greatly increased by illuminating samples deposited on transparent dielectrics at the substrates' Brewster angle. Using a commercial ellipsometer, the reflectivity of monolayers of CVD graphene is found to be up to 33 times higher than that of the substrate, i.e., an optical contrast as high as 3200% is obtained, more than 380 times higher than with standard optical microscopy. Also, with a simpler, homemade, experimental setup, a 1400% optical contrast was measured for a monolayer of CVD graphene and linear features as small as ~20 μm were visible in a monolayer, while ~6×17 μm^2 trilayers could still be imaged in exfoliated samples. It is also shown that the reflectance/transmittance ratio increases quadratically with the number of graphene layers, which may allow for counting layer numbers and identifying wrinkles and folds in transferred samples.

Keywords: Graphene, 2D materials, Brewster angle, optical contrast, transparent substrate.

1. Introduction

Since its isolation in 2004, graphene has been actively researched in fields as diverse as biosensing, energy storage, nanoelectronics and photonics/optoelectronics [1] for its numerous unique mechanical, chemical, electronic and optical properties [2-5]. The latter properties, in particular, have been determined via various methods [6-10] and are of particular importance for photonic and optoelectronic applications, in which case it is frequently necessary to deposit graphene on transparent substrates so that devices that exploit light in transmission can be developed. However, since graphene absorbs 2.3% and reflects <0.1% of normally incident visible light, optically identifying and inspecting graphene during optical experiments or photonic device development is a difficult task.

The visibility of graphene on a substrate is usually quantified via the obtained optical contrast, defined as [11-13]

$$C = \frac{R_g - R_S}{R_S}, \quad (1)$$

where R_g and R_S are the graphene and substrate reflectances, respectively. Typically, graphene and other 2D materials are optically detected and inspected by exploiting the optical contrast obtained on Si substrates containing a submicron layer of SiO_2 [11,14-17]. This layer plays the role of an etalon

and can interferometrically increase the contrast, with values up to 12% being reported [11,14]. The detection of graphene on transparent dielectric substrates, such as microscope slides, glass plates or touchscreens is a greater challenge since the contrast between the regions with and without graphene is significantly lower, on the order of 7% [13]. It has been shown that an interferometric increase in contrast can also be obtained in such substrates by depositing a layer of transparent polymer prior to the graphene deposition [18,19]. However, the interferometric layer invariably changes the substrate properties, which affects the characteristics of the device under study. In particular, this layer can alter the chemical potential of graphene, as well as significantly decrease the laser damage threshold of the sample, with the latter significantly limiting applications related to nonlinear optics.

This work aims at imaging graphene on transparent substrates with improved optical contrast without changing the substrate or the sample's physical/chemical properties. This is achieved through optically illuminating and imaging the sample at the substrate's Brewster angle. With CVD graphene, an exceptional optical contrast of up to 3200% was obtained for a single layer, being more than 380 times higher than that obtained in the same sample with standard optical microscopy. In exfoliated samples, trilayers of graphene could be identified, while bilayer and monolayer imaging would require improvements in the current experimental setup. The method is also able to identify the number of graphene layers in a sample, and may be applicable for other 2D materials.

2. Imaging graphene at Brewster angle

The Brewster angle is defined as the incidence angle for which reflection of *p*-polarized light on an interface between two dielectrics is extinguished. For an air-silicate glass interface, the Brewster angle has a value of ~57°. If, however, graphene is deposited onto the interface, its surface conductivity changes the electromagnetic boundary condition, allowing for some *p*-polarization reflection to take place. As has been shown [2,20], the real part of graphene's conductivity shifts the incidence angle for which *p*-polarization reflection is minimum (by ~0.5° towards a wider angle, for graphene on a silicate glass), while its small imaginary part makes the minimum reflection value non-zero (for which reason the minimum reflection angle is known as a *quasi*-Brewster angle). Therefore, as shown in Figure 1, if graphene partly covers a dielectric interface, *p*-polarized light that is incident at the substrate's Brewster angle will only be reflected where graphene is present. Analyzing Equation (1) for this case, it is noted that the substrate reflectivity will tend to zero, thus leading to an optical contrast that tends to infinity. Experimentally, the contrast will be limited by the dark current noise in the imaging system, imperfectly *p*-polarized light at the input and by stray light.

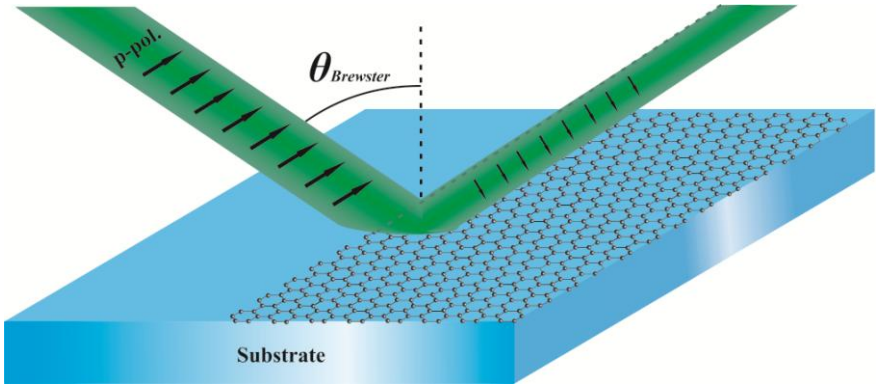

Figure 1. Schematic representation of *p*-polarized light being reflected solely on graphene when incidence takes place at the substrate's Brewster angle.

It is interesting to analyze the situation in which multiple graphene layers are deposited onto the dielectric substrate. A number of optical methods has been demonstrated to determine the exact number of deposited layers relying on the reflection [12,13,21], although none of them analyzed Brewster angle incidence. If we treat *N* layers of graphene as a surface presenting *N* times the

conductivity of graphene (σ_g) [3,13], the reflectance at the substrate's Brewster angle (R_g^B) for *p*-polarization at positions where graphene is present is given by [20]

$$R_g^B = \left|\frac{H_r^B}{H_i^B}\right|^2 = \left|\frac{\frac{4\pi}{\omega}N\sigma_g k_{1,z}k_{2,z}}{2\varepsilon_1 k_{2,z}+\frac{4\pi}{\omega}N\sigma_g k_{1,z}k_{2,z}}\right|^2 \approx \left(\frac{N\pi\alpha\cos\theta_1/2n_1}{1+N\pi\alpha\cos\theta_1/2n_1}\right)^2, \quad (2)$$

where ω is the angular frequency; $k_{1,z}$ is the substrate wave vector; $k_{2,z}$ is the superstrate wave vector; ε_1 and $n_1 = \varepsilon_1^{1/2}$ are the substrate dielectric constant and refractive index, respectively; α is the fine-structure constant; and θ_1 is the angle of refraction. Since in this case the *p*-polarization transmittance is given by [20]

$$T_g^B = \left|\frac{H_t^B}{H_i^B}\right|^2 = \left|\frac{2\varepsilon_1 k_{2,z}}{2\varepsilon_1 k_{2,z}+\frac{4\pi}{\omega}N\sigma_g k_{1,z}k_{2,z}}\right|^2 \approx \left(\frac{1}{1+N\pi\alpha\cos\theta_1/2n_1}\right)^2, \quad (3)$$

the R_g^B/T_g^B ratio is proportional to the square of the number of graphene layers:

$$\frac{R_g^B}{T_g^B} = \left|\frac{2\pi N\sigma_g k_{1,z}}{\varepsilon_1\omega}\right|^2 \approx (N\pi\alpha\cos\theta_1/2n_1)^2. \quad (4)$$

In equations (2) and (3) we used the fact that, at the Brewster angle, $\varepsilon_2 k_{1,z} = \varepsilon_1 k_{2,z}$, with ε_2 being the superstrate's dielectric constant. In equations (2) through (4) the last approximation assumes $\sigma_g \approx \sigma_0$, with the latter being graphene's universal conductivity [20]. As will be shown, this is indeed a good approximation for the experiments described here. From equation (4) one can see that the proposed imaging method not only is able to provide a high optical contrast between graphene and the optical substrate, but it is also expected to distinguish between different number of graphene layers. We note that all the analysis carried out here is valid for the visible wavelength range, away from van Hove singularities.

For the experimental demonstration of the method, the setup shown in Figure 2 was used. Broadband light is preferred, so as to avoid speckle. Therefore, for convenience, the optical source consisted of the first Raman Stokes of a 532-nm Q-switched Nd:YAG laser (0.3 ns pulse duration and 1 kHz repetition rate) that was generated in a 2.4-m multimode fiber; this source can, however, be replaced by any bright broadband source. A subsequent notch filter suppressed the remnant laser power resulting in a 2.7 nm FWHM spectrum centered at 545 nm. The coherence length [22] can be calculated to be ~50 μm, thus reducing the presence of speckle. The collimated green light was then linearly polarized using a Glan-laser calcite polarizer with nominal 50-dB extinction ratio and launched onto the sample with *p* polarization at the substrate's Brewster angle with an average power of 1 mW. An iris was used to reduce stray light and the sample was placed on a rotation stage so that the angle alignment could be optimized. The specular reflection from the sample was collected with either a 100-mm focal length lens or a 20× objective, depending on the desired magnification, and imaged onto a CCD camera. As the resulting images are captured at an oblique angle, they are contracted along one axis. To correct for this feature, distances along this axis were divided by $\cos(\theta_{Brewster})$. The intensity of all the images shown here are depicted in color scales, which were optimized to improve graphene's visibility in each case.

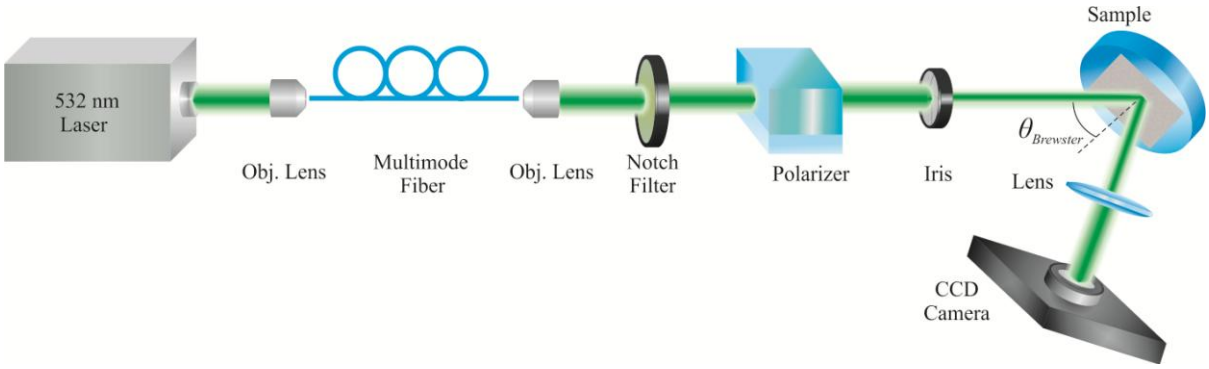

Figure 2. Experimental setup used for the Brewster angle imaging of graphene.

3. Sample preparation, results and analysis

The substrates used in the experiments were borosilicate microscope coverslips, which were found to present a Brewster angle of ~57º. They were cleaned via sequential acetone, isopropanol and deionized water baths in ultrasound for 15 minutes each before graphene deposition. Monolayers of CVD graphene were commercially obtained and then transferred to the glass substrates via the conventional wet-transfer process [23]. For investigating the reflectance dependence on the number of graphene layers, samples with 2 to 7 stacked graphene layers were fabricated via a modified wet-transfer method [23], in which during the transfer process monolayers of graphene are piled one upon the other up to the desired number of layers. Note that the method uses a single layer of PMMA independently of the number of graphene layers, so that contamination does not build up with the latter. Also to minimize contamination, all CVD samples were rinsed in two subsequent deionized water baths, for 4 hours each, after copper etching. After the transfer process, the PMMA layer was removed in a 30-minute anisole bath at room temperature and a 12-hour acetone bath at 50ºC, resulting in minimal PMMA residues. For comparison, the exact same transfer procedure was carried out using a copper foil without graphene, thus yielding a control sample that has all contaminants that result from the process, but has no graphene. Mechanically exfoliated samples were prepared, also on microscope coverslips, by exfoliating natural graphite with a sticky tape.

Figure 3 shows the R_g^B/T_g^B ratio as a function of the number of stacked CVD graphene layers. For this measurement the lens after the sample and the camera were replaced with an optical powermeter, while a second powermeter measured the power transmitted through the sample. A nearly quadratic growth of this ratio with the number of graphene layers can be observed, as expected from Equation (4), with an experimentally obtained exponent of 1.87±0.08 (with R^2 = 0.9895). In fact, since the reflected power in a graphene monolayer was as low as ~100 nW, thus being more affected by stray light, the first data point in the figure presents the greatest uncertainty. If this point is eliminated from the fitting procedure, the resulting fit (dashed line) leads to an exponent of 2.07±0.07 (with an improved R^2 = 0.9941), with an even better match to the parabola. Note, also, that taking the log of Equation (4), one gets $Y = log\left(\frac{R_g^B}{T_g^B}\right) \approx 2\log N + 2\log(\pi\alpha\ cos\theta_1/2n_1) = 2X - 4.40$, with n_1 = 1.52, which matches very closely the equation of the dashed line.

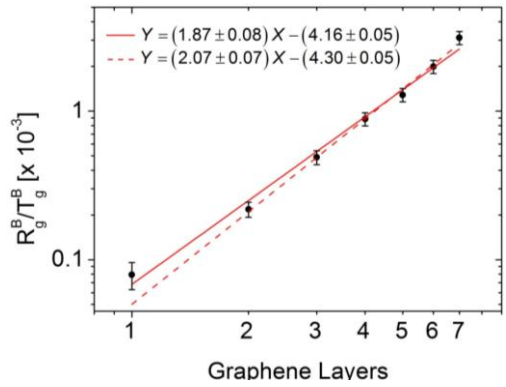

Figure 3. Reflection/transmission ratio for *p*-polarized light as a function of the number of stacked CVD graphene layers. Solid and dashed lines are linear fits to the experimental data.

Figure 4 compares the images of a CVD graphene monolayer obtained with conventional optical microscopy with those obtained with the present setup. Figure 4(a) shows the optical image obtained using a standard optical microscope, with a 10× objective. The regions corresponding to graphene, graphene border and substrate are identified as 1, 2, and 3, respectively. Illumination is provided in reflection and the condenser diaphragm is partially closed to improve graphene visualization. Regions 1 and 3 can hardly be distinguished and yield an optical contrast of 8.4% (the visibility of region 2 is increased by wrinkles and folds). Figure 4(b) shows images of two regions of the same sample obtained with the Brewster angle imaging setup (using a 100-mm focal length lens). Graphene is very

well distinguished from the bare substrate (darker shades of blue, indicating virtually no reflection). The images show that it is possible to observe the graphene fractures and folds, which can be exploited to access the quality of the transfer process. Ultrahigh contrasts of 1400% are calculated from these images (away from borders and wrinkles), which is more than 160 times the contrast obtained in Figure 4(a).

A number of tests was carried out to rule out the possibility that the high contrasts reported here are due to contamination from the graphene transfer process. Firstly, the control sample without graphene (but submitted to the complete transfer process) presented a contrast of only 10% between the region that received PMMA and the substrate. Secondly, we repeated the graphene transfer process with different polymers and obtained essentially the same optical contrast. Finally, we note that while PMMA was spin coated only once in each stacked graphene sample, the facts that the reflectivity increases quadratically with the number of graphene layers and that equation (4) fits very well to the experimental data in Figure 3 indicate, once again, that graphene, rather than PMMA contamination, is responsible for most of the observed reflectivity.

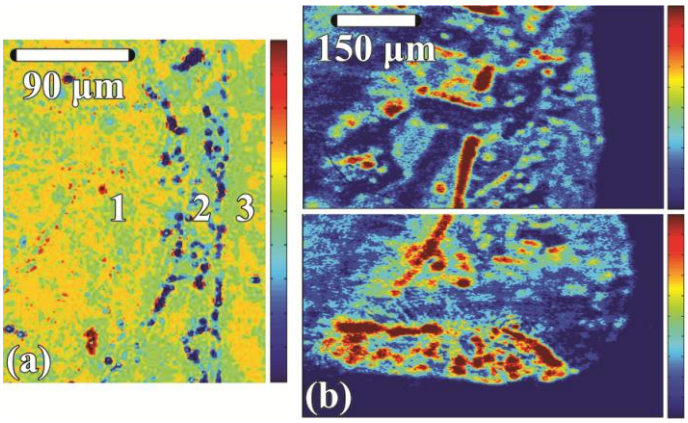

Figure 4. A monolayer CVD graphene sample imaged by (a) a conventional optical microscope (C = 8.4%), where 1, 2 and 3 are the graphene, graphene border and dielectric substrate regions respectively; and (b) Brewster angle imaging (C = 1400%).

In order to determine the variation of the optical contrast with the incidence angle, the reflectivity of a CVD graphene monolayer sample was measured with a commercial ellipsometer (Accurion's EP4). A diode laser at 658 nm was used in this case. The results for four representative angles are shown in Figure 5. At an angle of 50º, below the substrate's Brewster angle, Figure 5(a), both graphene and the substrate reflect similarly, yielding an optical contrast of 11.6%. At Brewster angle (found to be 56.7º), Figure 5(b), the substrate's reflection tends to zero and an optical contrast of 2600%, i.e, >300 times higher than with standard optical microscopy, is obtained. Figure 5(c) shows the image taken at graphene's *quasi*-Brewster angle, 57.3º, for which graphene's reflection is at its minimum. Interestingly, at this angle the substrate reflectance is still low and, thus, a very low contrast (~0.2%) is obtainted. Finally, at 58º, beyond the *quasi*-Brewster angle, the substrate's reflection increases, becoming lower than graphene's, Figure 5(d), which results in an optical contrast of -26.6%.

We note that the images shown in Figures 5(a)-(d) are affected by the reflection at the coverslip's opposite facet and by noise in the ellipsometer's imaging system. Contrast can, therefore, be improved through contacting the sample with a wedge, using index-matching fluid, and by noise level subtraction. Figure 5(e) shows the reflectivity obtained under these conditions on another CVD graphene monolayer sample, as well as on its glass substrate, as a function of the incidence angle (θ). The inset of the figure shows the corresponding contrast, which is as high as 3200% at the substrate's Brewster angle. The solid lines in the main part of Figure 5(e) are fittings of the form $f(\theta) = A.R_p(\theta) + B$, with A and B being free parameters and $R_p(\theta)$ being the p-polarization reflectance as a function of the incidence angle, whose form can be found in Ref. 20. The substrate's refractive index is left as a free parameter, with 1.518 and 1.528 yielding the best fits for the substrate and graphene

areas, respectively. For graphene, the total conductivity is assumed to be equal to graphene's universal conductivity, as varying this parameter within physically meaningful limits was found not to affect the fitting. For reflection on glass, the best fit was obtained with $A = 6.30\times10^4$ and $B = 0.47$, while for reflection on graphene $A = 9.55\times10^4$ and $B = 7.59$. While A is simply related to the incident light intensity (and, indeed, varied according to the experimental illumination of the sample), B indicates the amount of stray light that reaches the CCD camera. The fact that more stray light is present for reflection on graphene is believed to result from scattering (from wrinkle-induced surface roughness and residual contamination) and leads to the reduced contrast at graphene's *quasi*-Brewster angle. It also increases the contrast at the substrate's Brewster angle. If scattering on graphene were identical to that of the substrate (i.e., no contamination or additional roughness), a contrast 2.1× lower would be obtained, which is still two orders of magnitude higher than obtained with normal incidence illumination.

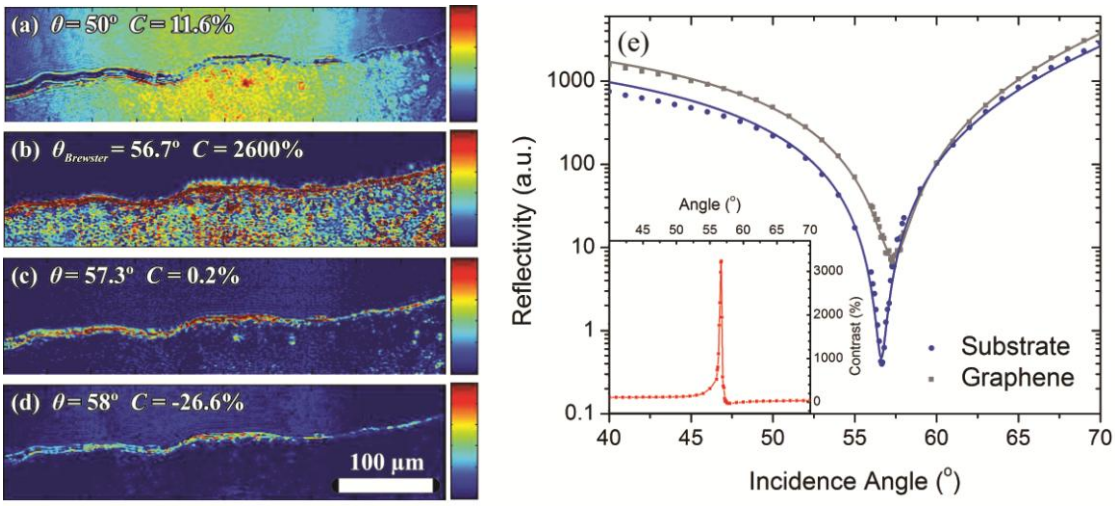

Figure 5. Results obtained with a commercial ellipsometer as a function of incidence/reflection angles on monolayer samples of CVD graphene. Images for incidence angles of (a) 50º (C = 11.6%); (b) 56.7º (substrate's Brewster angle; C = 2600%); (c) 57.3º (graphene's *quasi*-Brewster angle; C =0.2%); and (d) 58º (C = -26.6%). (e) Reflectivity as a function of the incidence angle on the substrate and on graphene. *Inset*: resulting contrast.

To demonstrate the ability to image smaller features with the homemade imaging setup, a pattern of lines was ablated from a CVD graphene monolayer sample by scanning a focused Q-switched Nd:YAG laser emitting 0.8 ns pulses at 1-kHz repetition rate and 1.06-µm wavelength. The resulting pattern is shown in Figure 6 both with confocal Raman mapping and with our Brewster angle setup. Figure 6(a) shows a map of the intensity of graphene's 2D Raman band, while Figure 6(b) is the Brewster angle image obtained with the 100-mm focal length lens. The ablated lines, which have thicknesses ranging from 5.2-µm to 21-µm, are easily recognized in both images. However, at these magnifications, the light intensity at the camera approaches the noise floor, decreasing the obtained contrast, which is now ~42%.

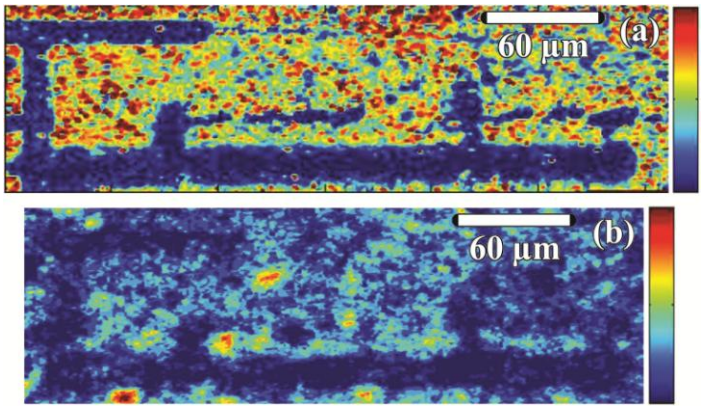

Figure 6. Images obtained by (a) confocal Raman mapping and (b) Brewster angle imaging of laser ablated lines on a monolayer CVD graphene.

At even higher magnifications (using the objective lens), small exfoliated graphene flakes can be imaged. Figure 7 shows images of an exfoliated sample with two regions of trilayer and one region of monolayer, as inferred by Raman spectroscopy. Figure 7(a) shows the 2D Raman band intensity mapping and Figure 7(b) shows the Brewster angle image. It can be seen that the ~6×17µm^2 trilayer graphene is optically imaged, presenting an optical contrast of 90%. Monolayers and bilayers could not be imaged in exfoliated flakes with the present setup because of the low intensities obtained at higher magnifications, as previously mentioned. However, we note that this limitation is not fundamental, since the method is in principle background-free, and can therefore be overcome with improved optics and electronics.

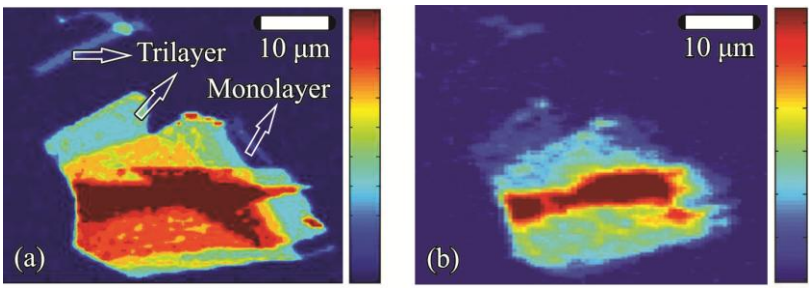

Figure 7. Images obtained by (a) confocal Raman mapping and (b) Brewster angle imaging of an exfoliated graphene flake.

5. Conclusion

Brewster angle imaging was introduced as an improved optical means to visualize graphene on transparent substrates. A drastic enhancement in the obtained optical contrast is demonstrated, with contrasts as high as 3200% (>380 factor) being measured for a monolayer of CVD graphene. A nearly quadratic growth on the reflectance/transmittance ratio with the number of graphene layers was measured, which may be exploited to identify wrinkles and folds in transferred graphene samples, as well as the number of layers in exfoliated flakes. The method may prove very attractive especially to inspect large surfaces of dielectrics covered with graphene. It is also expected to work with other 2D materials that are absorbing at the illumination wavelength, such as MoS_2 [24], which, thus, present a high real conductivity.

Acknowledgments

This work was funded by São Paulo Research Foundation (FAPESP), grant no. 2012/50259-8, CAPES-STINT collaboration program, CNPq, INCT FOTONICOM and MackPesquisa. P. Romagnoli

was supported by a CNPq scholarship. D. Lopez Cortes was supported by FINEP/CNPq. H. G. Rosa was supported by FAPESP scholarships, grant nos. 2010/19085-8 and 2012/07678-0. J. C. Viana-Gomes acknowledges financial support from the NRF-CRP grant R-144-000- 295-281 "Novel 2D materials with tailored properties - beyond graphene". The graphite used for obtaining exfoliated samples was kindly provided by Nacional de Grafite. The authors thank H. B. Ribeiro for useful discussion; H. X. P. Peixoto and R. Bentini for their help with ellipsometer measurements; and G. J. M. Fechine and F. Kessler for additional sample preparation with alternative polymers.

References

[1] Novoselov K S, Fal'ko V I, Colombo L, Gellert P R, Schwab M G and Kim K 2012 A roadmap for graphene *Nature* **490** 192-200.

[2] Stauber T, Peres N M R and Geim A K 2008 Optical conductivity of graphene in the visible region of the spectrum *Phys. Rev. B* **78** 085432.

[3] Bonaccorso F, Sun Z, Hasan T and Ferrari A C 2010 Graphene photonics and optoelectronics *Nat. Photonics* **4** 611-622.

[4] Castro Neto A H, Guinea F, Peres N M R, Novoselov K S and Geim A K 2009 The electronic properties of graphene *Rev. Mod. Phys.* **81** 109-162.

[5] Mattevi C, Eda G, Agnoli S, Miller S, Mkhoyan K A, Celik O, Mastrogiovanni D, Granozzi G, Garfunkel E and Chhowalla M 2009 Evolution of electrical, chemical, and structural properties of transparent and conducting chemically derived graphene thin films *Adv. Funct. Mater.* **19** 2577–2583.

[6] Wang X, Chen Y P and Nolte D D 2008 Strong anomalous optical dispersion of graphene: complex refractive index measured by Picometrology *Opt. Express* **16** 26 104113.

[7] Kravets V G, Grigorenko A N, Nair R R, Blake P, Anissimova S, Novoselov K S and Geim A K 2010 Spectroscopic ellipsometry of graphene and an exciton-shifted van Hove peak in absorption *Phys. Rev. B* 81 155413.

[8] Nelson F J, Kamineni V K, Zhang T, Comfort E S, Lee J U and Diebold A C 2010 Optical properties of large-area polycrystalline chemical vapor deposited graphene by spectroscopy ellipsometry *Appl. Phys. Lett.* **97** 253110.

[9] Zhang H, Virally S, Bao Q, Ping L K, Massar S, Godbout N and Kockaert P 2012 Z-scan measurement of the nonlinear refractive index of graphene Opt. Lett. 37 11 1856-1858.

[10] Cheon S, Kihm K D, Kim H G, Lim G, Park J S and Lee J S 2014 How to reliably determine the complex refractive index (RI) of graphene by using two independent measurement constraints *Sci. Rep.* **4** 6364.

[11] Blake P, Hill E W, Castro Neto A H, Novoselov K S and Jiang D 2007 Making graphene visible *Appl. Phys. Lett.* **91** 063124.

[12] Skulason H S, Gaskell P E and Szkopek T 2010 Optical reflection and transmission properties of exfoliated graphite from a graphene monolayer to several hundred graphene layers *Nanotechnology* **21** 295709.

[13] Gaskell P E, Skulason H S, Rodenchuk C and Szkopek T 2009 Counting graphene layers on glass via optical reflection microscopy *Appl. Phys.Lett.* **94** 143101.

[14] Bruna M and Borini S 2009 Optical constants of graphene layers in the visible range *Appl. Phys.Lett.* **94** 031901.

[15] Bruna M and Borini S 2009 Assessment of graphene quality by quantitative optical contrast analysis *J. Phys. D: Appl. Phys.* **42** 175307.

[16] Gorbachev R V, Riaz I, Nair R R, Jalil R, Britnell L, Belle B D, Hill E W, Novoselov K S, Watanabe K, Taniguchi T, Geim A K and Blake P 2011 Hunting for monolayer boron nitride: Optical and Raman signatures *Small* **7** 465–468.

[17] Castellanos-Gomez A, Agraït N and Rubio-Bollinger G 2010 Optical identification of atomically thin dichalcogenide crystals *Appl. Phys. Lett.* **96** 213116.

[18] Rosa H G, Viana-Gomes J C and Souza E A T de 2015 Transfer of exfoliated monolayer graphene flake onto optical fiber end face for erbium-doped fiber laser mode-locking *2D Materials*, **2** 031001.

[19] Dean C, Young A F, Wang L, Meric I, Lee G -H, Watanabe K, Taniguchi T, Shepard K, Kim P and Hone J 2012 Graphene based heterostructures *Solid State Commun.* **152** 1275-1282.

[20] Bludov Y V, Peres N M R and Vasilevskiy M I 2013 Unusual reflection of electromagnetic radiation from a stack of graphene layers at oblique incidence *J. Opt.* **15** 114004.

[21] Cheon S, Kihm K D, Park J S, Lee J S, Lee B J, Kim H and Hong B H 2012 How to optically count graphene layers *Opt. Lett.* **37** 3765-3767.

[22] Drexler W and Fujimoto J G 2008 *Optical coherence tomography* (Springer Berlin Heidelberg).

[23] Wang Y, Tong S W, Xu X F, Özyilmaz B and Loh K P 2011 Interface engineering of layer-by-layer stacked graphene anodes for high-performance organic solar cells *Adv. Mater.* **23** 1514–1518.

[24] Yim C, O'Brien M, McEvoy N, Winters S, Mirza I, Lunney J G and Duesberg G S 2014 Investigation of the optical properties of MoS2 thin films using spectroscopic ellipsometry *Appl. Phys. Lett.* **104** 103114.